

A Hidden Markov model for Bayesian data fusion of multivariate signals

Olivier Féron and Ali Mohammad-Djafari

Laboratoire des Signaux et Systèmes,
Unité mixte de recherche 8506 (CNRS-Supélec-UPS)
Supélec, Plateau de Moulon, 91192 Gif-sur-Yvette, France
emails = feron@lss.supelec.fr djafari@lss.supelec.fr

Abstract

In this work we propose a Bayesian framework for data fusion of multivariate signals which arises in imaging systems. More specifically, we consider the case where we have observed two images of the same object through two different imaging processes. The objective of this work is then to propose a coherent approach to combine these data sets to obtain a segmented image which can be considered as the fusion result of these two images.

The proposed approach is based on a Hidden Markov Modeling (HMM) of the images with common segmentation, or equivalently, with common hidden classification label variables which is modeled by the Potts Markov Random Field. We propose then an appropriate Markov Chain Monte Carlo (MCMC) algorithm to implement the method and show some simulation results and applications.

key words :

Data fusion, Classification and segmentation of Images, HMM, MCMC, Gibbs Algorithm.

1 Introduction

Data fusion and multi-source information has become a very active area of research in many domains : industrial nondestructive testing and evaluation ([1]), medical imaging [2, 3, 4], industrial inspection ([5])(quality control and condition monitoring) and security systems in general.

In all these areas, the main problem is how to combine the information contents of different sets of multivariate data $g_i(r)$. When the data set $g_i(r)$ is an image we have

$r \in \mathbf{R}^2$, and the problem becomes how to combine and represent their fusion. Very often the data sets g_i do not represent the same quantities. For example in medical imaging we have 2D radiographic data g_1 and echographical data g_2 which are related to different properties f_1 and f_2 of the body under examination by

$$g_i(r) = [H_i f_i](r) + \varepsilon_i(r) \quad (1)$$

where H_i are the operator functional of the measuring systems. We may note that estimating f_i given each set of data g_i is an inverse problem by itself which is often an ill-posed problem even if we may know perfectly the operator H_i . So very often people use the two data sets separately to obtain two images f_1 and f_2 and then they try to make a data fusion. We think it is possible to do a better job if we define more precisely what we mean by data fusion of two images f_1 and f_2 and if we try to use the data g_1 and g_2 to estimate directly not only f_1 and f_2 but also the common feature of them which we present by a third image z .

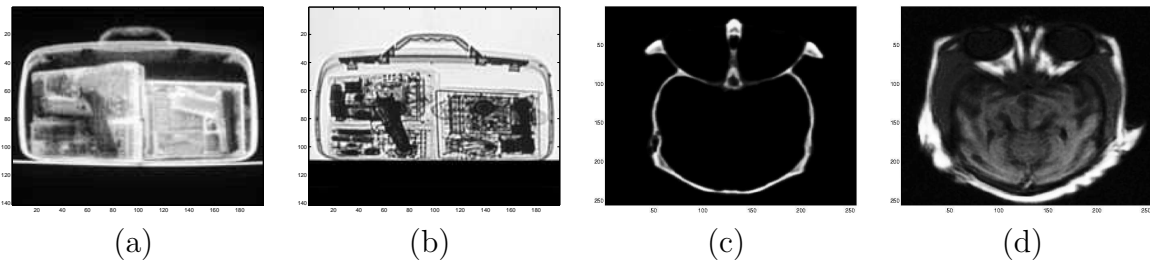


Figure 1: Examples of images for data fusion. a,b) two observations from transmission and backscattering X rays, c,d) MRI and CT images in medical imaging.

In this paper, to show the same ideas, we consider first the case where the two measuring systems can be assumed almost perfect which means that we can write

$$g_i(r) = f_i(r) + \varepsilon_i(r), \quad i = 1, 2 \quad (2)$$

and we focus on defining what we mean by a common feature z of the two images, how to model the relation between f_i and z and how to estimate f_1 , f_2 and z directly from the two data sets g_1 and g_2 .

The applications we have in mind in this work are either medical imaging or security systems imaging. As an example of the two data sets in the first application we consider MRI and CT images and as an example of the second application we consider a transmission and a backscattering diffusion images using X rays (see figure 1).

The rest of the paper is organized as follows : In section 2 we introduce the common feature z , model the relation between the images f_i to it through $p(f_i|z)$ and its proper characteristics through a prior law $p(z)$, and describe the Bayesian approach to estimate f_1 , f_2 and z through the *a posteriori* law $p(f_1, f_2, z|g_1, g_2)$. In section 3 we give some details on the selection of *a priori* probability laws $p(\theta)$ of the hyperparameters which define the *a posteriori* law $p(f_1, f_2, z|g_1, g_2)$. In section 4 we give detailed

expressions of the aforementioned *a posteriori* law and propose general structure of the MCMC algorithm to estimate f_1 , f_2 and z . Finally, in section 5 we present some simulation results to show the performances of the proposed method.

2 Modeling for data fusion

In this paper we consider the model (2) where after discretization and using the notations $\mathbf{g}_i = [g_i(1), \dots, g_i(S)]^T$, $\mathbf{f}_i = [f_i(1), \dots, f_i(S)]^T$ and $\boldsymbol{\varepsilon}_i = [\varepsilon_i(1), \dots, \varepsilon_i(S)]^T$ with S the total number of pixels of the images f_i , we have :

$$\mathbf{g}_i = \mathbf{f}_i + \boldsymbol{\varepsilon}_i, \quad i = 1, 2 \quad (3)$$

Within this model and assuming Gaussian independant noises, $p(\boldsymbol{\varepsilon}_i) = \mathcal{N}(0, \sigma_{\varepsilon_i}^2 \mathbf{I})$, we have

$$p(\mathbf{g}_1, \mathbf{g}_2 | \mathbf{f}_1, \mathbf{f}_2) = \prod_{i=1}^2 p(\mathbf{g}_i | \mathbf{f}_i) = \prod_{i=1}^2 p_{\varepsilon_i}(\mathbf{g}_i - \mathbf{f}_i)$$

As we want to reconstruct an image with statistically homogeneous regions, it is natural to introduce a hidden variable $\mathbf{z} = (z(1), \dots, z(S)) \in \{1, \dots, K\}^S$ which represents a common classification of the two images f_i . The problem is now to estimate the set of variables $(\mathbf{f}_1, \mathbf{f}_2, \mathbf{z})$ using the Bayesian approach :

$$\begin{aligned} p(\mathbf{f}_1, \mathbf{f}_2, \mathbf{z} | \mathbf{g}_1, \mathbf{g}_2) &= p(\mathbf{f}_1, \mathbf{f}_2 | \mathbf{z}, \mathbf{g}_1, \mathbf{g}_2) p(\mathbf{z} | \mathbf{g}_1, \mathbf{g}_2) \\ &\propto p(\mathbf{g}_1 | \mathbf{f}_1, \mathbf{z}) p(\mathbf{g}_2 | \mathbf{f}_2, \mathbf{z}) p(\mathbf{f}_1 | \mathbf{z}) p(\mathbf{f}_2 | \mathbf{z}) p(\mathbf{g}_1 | \mathbf{z}) p(\mathbf{g}_2 | \mathbf{z}) p(\mathbf{z}) \\ &\propto p(\mathbf{z}) \prod_{i=1}^2 p(\mathbf{g}_i | \mathbf{f}_i) p(\mathbf{f}_i | \mathbf{z}) p(\mathbf{g}_i | \mathbf{z}) \end{aligned}$$

Thus to be able to give an expression for $p(\mathbf{f}_1, \mathbf{f}_2, \mathbf{z} | \mathbf{g}_1, \mathbf{g}_2)$ we need to define $p(\mathbf{g}_i | \mathbf{f}_i)$, $p(\mathbf{f}_i | \mathbf{z})$, $p(\mathbf{g}_i | \mathbf{z})$ and $p(\mathbf{z})$.

Assuming $\boldsymbol{\varepsilon}_i$ centered, white and Gaussian, we have :

$$p(\mathbf{g}_i | \mathbf{f}_i) = \mathcal{N}(\mathbf{g}_i - \mathbf{f}_i, \sigma_{\varepsilon_i}^2 \mathbf{I})$$

To assign $p(\mathbf{f}_i | \mathbf{z})$ we first define the sets of pixels which are in the same class :

$$\begin{aligned} R_k &= \{r : z(r) = k\}, & |R_k| &= n_k \\ \mathbf{f}_{i_k} &= \{f_i(r) : z(r) = k\} \end{aligned}$$

Then we assume that all the pixels of an image f_i which are in the same class will be characterized by a mean m_{i_k} and a variance $\sigma_{i_k}^2$:

$$p(f_i(r) | z(r) = k) = \mathcal{N}(m_{i_k}, \sigma_{i_k}^2)$$

With these notations we have :

$$\begin{aligned}
p(\mathbf{f}_{i_k}) &= \mathcal{N}(m_{i_k}\mathbf{1}, \sigma_{i_k}^2\mathbf{I}) \\
p(\mathbf{f}_i|\mathbf{z}) &= \prod_{k=1}^K (m_{i_k}\mathbf{1}, \sigma_{i_k}^2\mathbf{I}) \\
&= \prod_{k=1}^K \left(\frac{1}{\sqrt{2\pi\sigma_{i_k}^2}} \right)^{n_k} \exp \left\{ -\frac{1}{2\sigma_{i_k}^2} \|\mathbf{f}_{i_k} - m_{i_k}\mathbf{1}\|^2 \right\}, \quad i = 1, 2.
\end{aligned}$$

The next step is to define $p(\mathbf{g}_i|\mathbf{z})$. To do this we may use the relation (3) and the laws $p(\mathbf{f}_i|\mathbf{z})$ and $p(\boldsymbol{\varepsilon}_i)$ to obtain

$$p(g_i(r)|z(r) = k) = \mathcal{N}(m_{i_k}, \sigma_{i_k}^2 + \sigma_{\varepsilon_i}^2),$$

Finally we have to assign $p(\mathbf{z})$. As we introduced the hidden variable \mathbf{z} for finding statistically homogeneous regions in images, it is natural to define a spatial dependance on these labels. The simplest model to account for this desired local spatial dependancy is a Potts Markov Random Field model :

$$p(\mathbf{z}) = \frac{1}{T(\alpha)} \exp \left\{ \alpha \sum_{r \in \mathcal{S}} \sum_{s \in \mathcal{V}(r)} \delta(z(r) - z(s)) \right\},$$

where \mathcal{S} is the set of pixels, $\delta(0) = 1$, $\delta(t) = 0$ si $t \neq 0$, $\mathcal{V}(r)$ denotes the neighborhood of the pixel r (here we consider a neighborhood of 4 pixels) and α represents the degree of the spatial dependance of the variable \mathbf{z} . If $\alpha = 0$ then the labels \mathbf{z} are considered as independant variables. On the other hand if $\alpha > 1$ then we give a strong *a priori* of a little number of great homogeneous regions. A good compromise is to choose *a priori* α between 0,3 and 0,9.

We have now all the necessary prior laws $p(\mathbf{g}_i|\mathbf{f}_i)$, $p(\mathbf{f}_i|z)$, $p(\mathbf{g}_i|z)$ and $p(\mathbf{z})$ and then we can give an expression for $p(\mathbf{f}_1, \mathbf{f}_2, \mathbf{z}|\mathbf{g}_1, \mathbf{g}_2)$. However these probability laws have in general unknown parameters such as $\sigma_{\varepsilon_i}^2$ in $p(\mathbf{g}_i|\mathbf{f}_i)$ or m_{i_k} and $\sigma_{i_k}^2$ in $p(\mathbf{f}_i|z)$. In a full Bayesian approach, we have to assign prior laws to these "hyperparameters". This point is addressed in the next section.

3 Prior selection of the hyperparameters

There is an extensive litterature on the construction of non informative priors. In this section we use results from [6] to choose particular priors, taking into account the restriction of our particular parametrical model. In [6] the authors used differential geometry tools to construct particular priors.

Let $\mathbf{m}_i = (m_{ik})_{k=1,\dots,K}$ and $\boldsymbol{\sigma}_i^2 = (\sigma_{ik}^2)_{k=1,\dots,K}$ be the means and the variances of the pixels in different regions of the images \mathbf{f}_i as defined before. We define $\boldsymbol{\theta}_i$ as the set of all the parameters which must be estimated :

$$\boldsymbol{\theta}_i = (\sigma_{\varepsilon_i}^2, \mathbf{m}_i, \boldsymbol{\sigma}_i^2), \quad i = 1, 2$$

We choose the prior distribution of $\boldsymbol{\theta}_i$ of the following form :

$$\pi(\boldsymbol{\theta}) \propto e^{-CD_\delta(p_{\boldsymbol{\theta}}, p_0)} \sqrt{\|g(\boldsymbol{\theta})\|},$$

where $p_{\boldsymbol{\theta}}$ is the likelihood of $\boldsymbol{\theta}$, p_0 is a reference distribution, C is a constant which represents the confidence degree we have on p_0 , D_δ is the δ -divergence and g is the Fisher information matrix.

The authors in ([6]) showed that if we choose this prior distribution for $\boldsymbol{\theta}_i$ with $\delta = 0$, we find the conjugate priors. When applied those results for our case, where these priors become :

- Inverse Gamma $\mathcal{IG}(\alpha_{i0}, \beta_{i0})$ for the variances $\sigma_{\varepsilon_i}^2$ and σ_{ik}^2 ,
- Gaussian $\mathcal{N}(m_{i0}, \sigma_{i0}^2)$ for the means m_{ik} .

The hyper-hyperparameters α_{i0} , β_{i0} , m_{i0} and σ_{i0}^2 are fixed and the results are not in general too sensitive to their exact values.

4 *a posteriori* distributions for the Gibbs algorithm

The Bayesian approach consists now to estimate the whole set of variables $(\mathbf{f}_1, \mathbf{f}_2, \mathbf{z}, \boldsymbol{\theta}_1, \boldsymbol{\theta}_2)$ following the joint *a posteriori* distribution $p(\mathbf{f}_1, \mathbf{f}_2, \mathbf{z}, \boldsymbol{\theta}_1, \boldsymbol{\theta}_2 | \mathbf{g}_1, \mathbf{g}_2)$. It is difficult to simulate a joint sample $(\hat{\mathbf{f}}_1, \hat{\mathbf{f}}_2, \hat{\mathbf{z}}, \hat{\boldsymbol{\theta}}_1, \hat{\boldsymbol{\theta}}_2)$ directly from his joint *a posteriori* distribution. However we can note that considering the prior laws defined before, we are able to simulate the conditionnal *a posteriori* laws $p(\mathbf{f}_1, \mathbf{f}_2, \mathbf{z} | \mathbf{g}_1, \mathbf{g}_2, \boldsymbol{\theta}_1, \boldsymbol{\theta}_2)$ and $p(\boldsymbol{\theta}_1, \boldsymbol{\theta}_2 | \mathbf{g}_1, \mathbf{g}_2, \mathbf{f}_1, \mathbf{f}_2, \mathbf{z})$. That's why we propose a Gibbs algorithm to estimate $(\hat{\mathbf{f}}_1, \hat{\mathbf{f}}_2, \hat{\mathbf{z}}, \hat{\boldsymbol{\theta}}_1, \hat{\boldsymbol{\theta}}_2)$, decomposing this set of variables into two subsets, $(\mathbf{f}_1, \mathbf{f}_2, \mathbf{z})$ and $(\boldsymbol{\theta}_1, \boldsymbol{\theta}_2)$. Then the Gibbs algorithm follows : given an initial state $(\hat{\boldsymbol{\theta}}_1, \hat{\boldsymbol{\theta}}_2)^{(0)}$,

Gibbs sampling

repeat until convergence

1. simulate $(\hat{\mathbf{f}}_1^{(n)}, \hat{\mathbf{f}}_2^{(n)}, \hat{\mathbf{z}}^{(n)}) \sim p(\mathbf{f}_1, \mathbf{f}_2, \mathbf{z} | \mathbf{g}_1, \mathbf{g}_2, \hat{\boldsymbol{\theta}}_1^{(n-1)}, \hat{\boldsymbol{\theta}}_2^{(n-1)})$
 2. simulate $\hat{\boldsymbol{\theta}}_i^{(n)} \sim p(\boldsymbol{\theta}_i | \mathbf{g}_i, \hat{\mathbf{f}}_i^{(n)}, \hat{\mathbf{z}}^{(n)})$
-

We will now define the conditionnal *a posteriori* distribution we use for the Gibbs algorithm.

sampling $\boldsymbol{\theta}_i | \mathbf{f}_i, \mathbf{g}_i, \mathbf{z}$:

We have the following relation :

$$p(\boldsymbol{\theta}_i | \mathbf{f}_i, \mathbf{g}_i, \mathbf{z}) \propto p(\sigma_{\varepsilon_i}^2 | \mathbf{f}_i, \mathbf{g}_i) p(\mathbf{m}_i, \boldsymbol{\sigma}_i^2 | \mathbf{f}_i, \mathbf{z})$$

Those *a posteriori* distributions are calculated from the prior selection fixed before and we have

- $m_{ik} | \mathbf{f}_i, \mathbf{z}, \sigma_{ik}^2, m_{i0}, \sigma_{i0}^2 \sim \mathcal{N}(\mu_{ik}, v_{ik}^2)$, with

$$\mu_{ik} = v_{ik}^2 \left(\frac{m_{i0}}{\sigma_{i0}^2} + \frac{1}{\sigma_{ik}^2} \sum_{r \in R_k} f_i(r) \right)$$

$$v_{ik}^2 = \left(\frac{n_k}{\sigma_{ik}^2} + \frac{1}{\sigma_{i0}^2} \right)^{-1}$$

- $\sigma_{ik}^2 | \mathbf{f}_i, \mathbf{z}, \alpha_{i0}, \beta_{i0} \sim \mathcal{IG}(\alpha_{ik}, \beta_{ik})$, with

$$\alpha_{ik} = \alpha_{i0} + \frac{n_k}{2}$$

$$\beta_{ik} = \beta_{i0} + \frac{s_i}{2}$$

where $s_i = \sum_{r \in R_k} f_i(r)^2 - n_k \bar{f}_i^2$, $\bar{f}_i = \frac{1}{n_k} \sum_{r \in R_k} f_i(r)$

- $\sigma_{\varepsilon_i}^2 | \mathbf{f}_i, \mathbf{g}_i \sim \mathcal{IG}(\nu_i, \Sigma_i)$, with

$$\nu_i = \frac{S}{2}, \quad S = \text{total number of pixels}$$

$$\Sigma_i = \frac{S}{2} \left(R_{\mathbf{g}_i \mathbf{g}_i} - \frac{R_{\mathbf{g}_i \mathbf{f}_i}^2}{R_{\mathbf{f}_i \mathbf{f}_i}} \right)$$

where $R_{xy} = \frac{1}{S} \sum_r x(r) y^*(r)$.

Sampling $\mathbf{f}_1, \mathbf{f}_2, \mathbf{z} | \mathbf{g}_1, \mathbf{g}_2, \boldsymbol{\theta}_1, \boldsymbol{\theta}_2$:

Using the Bayes formula we have :

$$p(\mathbf{f}_1, \mathbf{f}_2, \mathbf{z} | \mathbf{g}_1, \mathbf{g}_2, \boldsymbol{\theta}_1, \boldsymbol{\theta}_2) = p(\mathbf{f}_1, \mathbf{f}_2 | \mathbf{z}, \mathbf{g}_1, \mathbf{g}_2, \boldsymbol{\theta}_1, \boldsymbol{\theta}_2) p(\mathbf{z} | \mathbf{g}_1, \mathbf{g}_2, \boldsymbol{\theta}_1, \boldsymbol{\theta}_2)$$

Then the sampling of this joint distribution is again obtained through a Gibbs sampling scheme and then $p(\mathbf{f}_i | \mathbf{g}_i, \mathbf{z}, \boldsymbol{\theta}_i)$ by sampling first $p(\mathbf{z} | \mathbf{g}_1, \mathbf{g}_2, \boldsymbol{\theta}_1, \boldsymbol{\theta}_2)$. For the first step we have :

$$\begin{aligned} p(\mathbf{z} | \mathbf{g}_1, \mathbf{g}_2, \boldsymbol{\theta}_1, \boldsymbol{\theta}_2) &\propto p(\mathbf{g}_1, \mathbf{g}_2 | \mathbf{z}, \boldsymbol{\theta}_1, \boldsymbol{\theta}_2) p(\mathbf{z}) \\ &= p(\mathbf{g}_1 | \mathbf{z}, \boldsymbol{\theta}_1) p(\mathbf{g}_2 | \mathbf{z}, \boldsymbol{\theta}_2) p(\mathbf{z}) \end{aligned}$$

and for the next step we have :

$$p(f_i(r)|g_i(r), z(r) = k, \boldsymbol{\theta}_i) = \mathcal{N}(m_{ik}^{apost}, \sigma_{ik}^{2apost})$$

where

$$\begin{aligned} \sigma_{ik}^{2apost} &= \left(\frac{1}{\sigma_{\varepsilon_i}^2} + \frac{1}{\sigma_{ik}^2} \right)^{-1} \\ m_{ik}^{apost} &= \sigma_{ik}^{2apost} \left(\frac{g_i(r)}{\sigma_{\varepsilon_i}^2} + \frac{m_{ik}}{\sigma_{ik}^2} \right). \end{aligned}$$

As we choosed a Potts Markov Random Field model for the labels, we may note that an exact sampling of the *a posteriori* distribution $p(\mathbf{z}|\mathbf{g}_1, \mathbf{g}_2, \boldsymbol{\theta}_1, \boldsymbol{\theta}_2)$ is impossible. In theory, in each step, we have to implement again a third Gibbs sampling to obtain exact samples of $\hat{\mathbf{z}}$. However this will increase significantly the complexity of the algorithm. To obtain a faster algorithm, the solution we propose consists in implementing only one cycle of the Gibbs sampling for \mathbf{z} in each iteration. In fact it comes down to decompose the set of variables into three subsets $(\boldsymbol{\theta}_1, \boldsymbol{\theta}_2)$, $(\mathbf{f}_1, \mathbf{f}_2)$, and \mathbf{z} . The Gibbs algorithm we propose is then : given an initial state $(\hat{\boldsymbol{\theta}}_1, \hat{\boldsymbol{\theta}}_2, \hat{\mathbf{z}})^{(0)}$,

Gibbs sampling

repeat until convergence

1. simulate $\hat{\mathbf{z}}^{(n)} \sim p(\mathbf{z}|\hat{\mathbf{z}}^{(n-1)}, \mathbf{g}_1, \mathbf{g}_2, \hat{\boldsymbol{\theta}}_1^{(n-1)}, \hat{\boldsymbol{\theta}}_2^{(n-1)})$
 simulate $\hat{\mathbf{f}}_i^{(n)} \sim p(\mathbf{f}_i|\mathbf{g}_i, \hat{\mathbf{z}}^{(n)}, \hat{\boldsymbol{\theta}}_i^{(n-1)})$
 2. simulate $\hat{\boldsymbol{\theta}}_i^{(n)} \sim p(\boldsymbol{\theta}_i|\hat{\mathbf{f}}_i^{(n)}, \hat{\mathbf{z}}^{(n)}, \mathbf{g}_i)$
-

As we choosed a first order neighborhood system for the labels, we may also note that it is possible to implement the Gibbs algorithm in parallel. Indeed, we can decompose the whole set of pixels into two subsets forming a chessboard (see figure 2). In this case if we fix the black (respectively white) labels, then the white (respectively black) labels become independant.

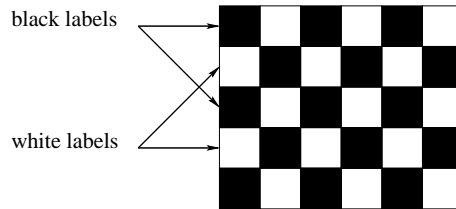


Figure 2: Chessboard decomposition of the labels \mathbf{z}

This decomposition reduces the complexity of the Gibbs algorithm because we can simulate the whole set of labels in only two steps. The Parallel Gibbs algorithm we implemented is then the following : given an initial state $(\hat{\boldsymbol{\theta}}_1, \hat{\boldsymbol{\theta}}_2, \hat{\mathbf{z}})^{(0)}$,

Parallel Gibbs sampling

repeat until convergence

1. simulate $\hat{\mathbf{z}}_N^{(n)} \sim p(\mathbf{z}|\hat{\mathbf{z}}_B^{(n-1)}, \mathbf{g}_1, \mathbf{g}_2, \hat{\boldsymbol{\theta}}_1^{(n-1)}, \hat{\boldsymbol{\theta}}_2^{(n-1)})$
 simulate $\hat{\mathbf{z}}_B^{(n)} \sim p(\mathbf{z}|\hat{\mathbf{z}}_N^{(n)}, \mathbf{g}_1, \mathbf{g}_2, \hat{\boldsymbol{\theta}}_1^{(n-1)}, \hat{\boldsymbol{\theta}}_2^{(n-1)})$
 simulate $\hat{\mathbf{f}}_i^{(n)} \sim p(\mathbf{f}_i|\mathbf{g}_i, \hat{\mathbf{z}}^{(n)}, \hat{\boldsymbol{\theta}}_i^{(n-1)})$
2. simulate $\hat{\boldsymbol{\theta}}_i^{(n)} \sim p(\boldsymbol{\theta}_i|\hat{\mathbf{f}}_i^{(n)}, \hat{\mathbf{z}}^{(n)}, \mathbf{g}_i)$

In the following we have implemented this algorithm.

5 Simulation and results

Here we illustrate two applications of the proposed method in cases of medical imaging and security systems. The first application is MRI and CT images of a brain which are (256 X 256) images.

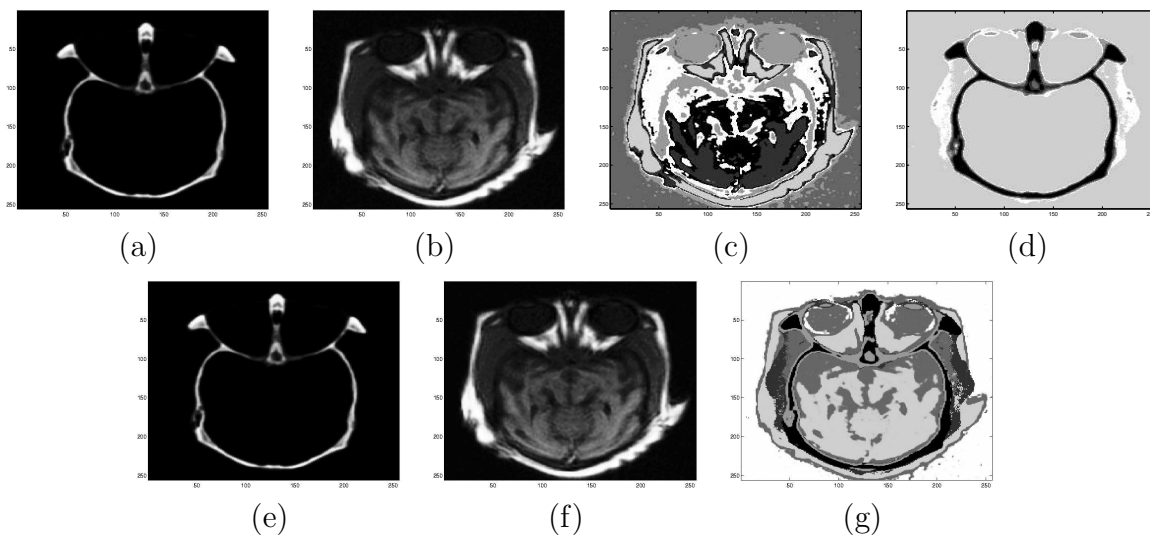


Figure 3: Results of data fusion from MRI and CT images. a,b) MRI and CT images in medical imaging. c,d) respective segmentation of the two images taken independantly. e,f) respective reconstruction of the images. g) result of data fusion.

Figure 3 shows the data fusion result of the proposed method comparing independant segmentation of the two images and segmentation using data fusion. As it is seen on this figure the fusionned segmentation we obtain contains all the regions and boundaries of both images. This is particularly visible in the up-center of the image. The second application is X ray transmission and backscattering images, which are (141 X 192) images. The observed object is a suitcase containing two guns. Figure 4 shows the result of the proposed method. The independant segmentation of the X ray backscattering image show clearly the presence of the right gun, but it is difficult to distinguish the left gun whatever the number of labels. In this figure we can see that

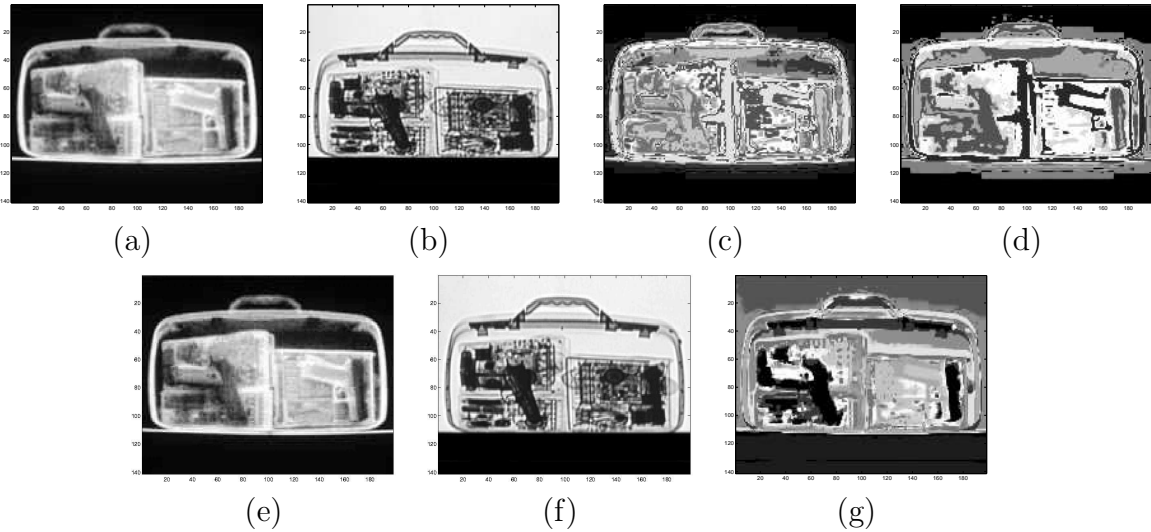


Figure 4: Results of data fusion from X ray images. a,b) two observations from transmission and backscattering X rays. c) segmentation of image a) only with 8 labels. d) segmentation of image a) only with 7 labels. e,f) respective reconstruction of the images. g) result of data fusion.

the X ray transmission image brings essential information to precisely distinguish the left gun without eliminating the detection of the one on the right.

In both applications we have satisfactoring results of image fusion, even when images present a great number of homogeneous regions and boundaries. Figures 3 and 4 show that the proposed method uses both images to increase the performances of the segmentation. Note also that the segmentation time of one image independantly or as result of the image fusion is practically the same. Indeed the proposed method does not really increase the complexity, making fusion and reconstruction in the same time.

However in both cases the reconstructed images are not visibly improved. This is mostly due to the assumption that the values of $f_i(r)$ at any two different pixels are independant. We may expect for better results of reconstruction and segmentation if we introduce some local spatial dependancy between the neighboring pixels of images $f_i(r)$. This point is under developpment and we will report soon on the results.

6 Conclusion

We proposed a Bayesian method for data fusion of images, with a Potts Markov Random Field model on the hidden variable z . We illustrated how the segmentation is improved by using data fusion through two applications : MRI and CT images in medical imaging and X ray transmission and backscattering images in security systems.

We showed then how reconstruction and fusion can be computed in the same time

using a MCMC algorithm, which reduce the complexity of the algorithm.

References

- [1] S. Gautier, G. Le Besnerais, A. Mohammad-Djafari, and B. Lavayssière, *Data fusion in the field of non destructive testing*. Maximum Entropy and Bayesian Methods, Santa Fe, NM: Kluwer Academic Publ., K. Hanson ed., 1995.
- [2] J. Boyd and J. Little, “Complementary data fusion for limited-angle tomography,” in *IEEE Proceeding of Computer vision and Pattern recognition*, (Seattle), pp. 288–294, 1994.
- [3] J. Boyd, “Limited-angle computed tomography for sandwich structures using data fusion,” in *journal of Nondestructive Evaluation*, vol.14, no.2, pp. 61–76, 1995.
- [4] G. Matsopoulos, S. Marshall, and J. Brunt, “Multiresolution morphological fusion of mr and ct images of the human brain,” in *IEEE Proceedings on Vision, Image and Signal Processing*, vol.141 Issue : 3, (Seattle), pp. 137–142, 1994.
- [5] T. Bass, “Intrusion detection systems and multisensor data fusion,” in *Comm. of the ACM*, vol. 43, pp. 99–105, 2000.
- [6] H. Snoussi and A. Mohammad-Djafari, “Information Geometry and Prior Selection.,” in *Bayesian Inference and Maximum Entropy Methods* (C. Williams, ed.), pp. 307–327, MaxEnt Workshops, American Institute of Physics, August 2002.
- [7] G. Gindi, M. Lee, A. Rangarajan, and I. G. Zubal, “Bayesian reconstruction of functional images using anatomical information as priors,” *IEEE Transactions on Medical Imaging*, vol. 12, no. 4, pp. 670–680, 1993.
- [8] S. Gautier, J. Idier, A. Mohammad-Djafari, and B. Lavayssière, “X-ray and ultrasound data fusion,” in *Proceedings of the International Conference on Image Processing*, (Chicago, IL), pp. 366–369, October 1998.
- [9] T. Hebert and R. Leahy, “A generalized EM algorithm for 3-D Bayesian reconstruction from Poisson data using Gibbs priors,” *IEEE Transactions on Medical Imaging*, vol. 8, pp. 194–202, June 1989.
- [10] D. Geman and G. Reynolds, “Constrained restoration and the recovery of discontinuities,” *IEEE Transactions on Pattern Analysis and Machine Intelligence*, vol. 14, pp. 367–383, March 1992.
- [11] G. Aubert and L. Vese, “A variational method in image recovery,” *SIAM Journal of Numerical Analysis*, vol. 34, pp. 1948–1979, October 1997.
- [12] P. Charbonnier, L. Blanc-Féraud, G. Aubert, and M. Barlaud, “Deterministic edge-preserving regularization in computed imaging,” *IEEE Transactions on Image Processing*, vol. 6, pp. 298–311, February 1997.
- [13] C. Robert, *Méthodes de Monte-Carlo par chaînes de Markov*. Paris, France: Economica, 1996.